M&C 2017 - International Conference on Mathematics & Computational Methods Applied to Nuclear Science & Engineering, Jeju, Korea, April 16-20, 2017, on USB (2017)

Spectral Analysis for Convergence Assessment in Monte Carlo Criticality Calculation

Taro Ueki

Japan Atomic Energy Agency, Nuclear Safety Research Center, Criticality Safety Research Group: 2-4 Shirakata-Shirane, Tokai-Mura, Naka-Gun, Ibaraki-Ken 319-1195, Japan, ueki.taro@jaea.go.jp

Abstract - *In Monte Carlo criticality calculation, the formation of a confidence interval is based on the central limit theorem (CLT) for a series of tallies from generations in equilibrium. A fundamental assertion resulting from CLT is the convergence in distribution (CID) of an interpolated standardized time series (ISTS) of tallies. This work reports a spectral analysis approach to ISTS in order to assess the convergence of tallies in terms of CID. Numerical results are demonstrated for a preliminary model of uranium-concrete debris.*

I. INTRODUCTION

In Monte Carlo (MC) criticality calculation, the formation of a confidence interval is based on the central limit theorem[1] (CLT) for a series of tallies from generations in equilibrium. A fundamental assertion resulting from CLT is the weak convergence of an interpolated standardized time series (ISTS) of tallies formulated as the convergence in distribution (CID).[2] In this work, the spectral analysis with power spectrum computation was applied to ISTS in order to assess the convergence of tallies in terms of CID. Numerical results are demonstrated for a preliminary model of UO_2-concrete debris.[3] These results are interpreted compared with the reference power spectrum of Brownian motion.

A significant amount of research has been conducted on the standard deviation estimation of the sample mean of tallies as testified in extensive literature citations in recent works.[4,5] Many estimators were investigated in these works in order to incorporate or exclude the influence of correlation. However, no attempt was made at convergence assessment in the framework of CID. Currently, a reference methodology is not available concerning how to measure the converged state of distribution. For this reason, it is worthwhile investigating the spectral analysis of ISTS with power spectrum computation. If contrasted with the spectral analysis approach to MC fission source distribution[6], the availability of the reference stochastic processes of Brownian motion and Brownian bridge is a unique and noble aspect in this work.

II. CENTRAL LIMIT THEOREM AND SPECTRAL ANALYSIS

In MC criticality calculation, a fission source generation in equilibrium is iterated in a form of the power method with particle population normalization. Consequently, the generations yield a correlated series of tallies denoted as $x_1, x_2, \ldots, x_n$ for which the joint statistical property of x_j and x_k is the same as that of x_{j+h} and x_{k+h}. Here, the subscripts denote generation numbers, n is the total number of generations run through equilibrium, and h is generation shift. The tally x is estimated by the sample mean of $x_1, x_2, \ldots, x_n$ and the variance of this estimate is

$$\frac{1}{n}\left[AC(0)+2\sum_{j=1}^{n-1}\left(1-\frac{j}{n}\right)AC(j)\right] \approx \frac{\sigma^2}{n} \equiv \frac{1}{n}\left[AC(0)+2\sum_{j=1}^{n-1}AC(j)\right], \qquad (1)$$

where $AC(j)$ is the autocovariance of x_k and x_{k+j} and n is assumed to be sufficiently large in terms of the attenuation of $AC(j)$. To proceed, it is convenient to introduce the partial sample mean of $x_1, x_2, \ldots, x_n$ for the first m generations as

$$ps_m \equiv \frac{1}{m}\sum_{j=1}^{m} x_j\ ,\ 1 \le m \le n\,. \qquad (2)$$

Denoting the true mean/expected value of x_i as μ, a form of CLT reads[2,7]

$$\frac{\lfloor nt \rfloor\left(ps_{\lfloor nt \rfloor}-\mu\right)}{\sigma\sqrt{n}} \rightarrow_D B_M(t) \qquad (3)$$

for $0 \le t \le 1$ as $n \rightarrow \infty$, where $\lfloor nt \rfloor$ is the largest integer not exceeding nt, $\rightarrow_D$ stands for CID and $B_M(t)$ is the path of Brownian motion. A fundamental assertion derived from the CLT in Eq (3) is[2,7]

$$T_n(t) \equiv \frac{\lfloor nt \rfloor(ps_n - ps_{\lfloor nt \rfloor})}{\sigma\sqrt{n}} \rightarrow_D B_B(t) \equiv B_M(t) - tB_M(1) \qquad (4)$$

for $0 \le t \le 1$ as $n \rightarrow \infty$, where $T_n(t)$ is ISTS referred to in Sec. I, $B_B(t)$ is known as the path of Brownian bridge. In Eq (4), $T_n(m/n) = m(ps_n - ps_m)/(\sigma n^{1/2})$, $m=0,1,\ldots,n$, is called the standardized time series of tallies. In MC criticality calculation, the convergence theorem in Eq (4) has been utilized for the variance estimation with orthonormally weighted standardized time series (OWSTS).[4,7] In the OWSTS methodology, weighting functions are introduced as

$$w_j^C(t) = \sqrt{8}\pi j\cos(2\pi jt),\ \ j = 1,2,\ldots,$$
$$w_j^S(t) = \sqrt{8}\pi j\sin(2\pi jt),\ \ j = 1,2,\ldots, \qquad (5)$$

and a statistic is defined as

$$Z_j^F(n) \equiv \frac{1}{n}\sum_{m=1}^{n-1} w_j^F\left(\frac{m}{n}\right)\sigma T_n\left(\frac{m}{n}\right),\ F = C,S,\ j = 1,2,\ldots. \qquad (6)$$

Note that σ in front of T_n and σ in the denominator of T_n cancel each other. The variance of sample mean is then computed as

$$\mathrm{var}[ps_n] = \frac{\sigma^2}{n} \approx \frac{1}{2nJ}\sum_{j=1}^{J}\left[(Z_j^C(n))^2 + (Z_j^S(n))^2\right], \qquad (7)$$

where J is the order of pairs of weighting functions. The OWSTS estimator in Eq (7) was demonstrated to be unbiased if n is sufficiently large.[4] However, in order to ensure the reliability of tally estimation, the condition of "n is sufficiently large" should be characterized by some measurable criterion.

Brownian motion in Eqs (3) and (4) is a special case of fractional Brownian motion (FBM). The power spectrum of FBM was argued and established in previous works[8,9], which yielded

$$S_{BM}(f) = \frac{1}{f^2},\ \ f\text{: frequency (s}^{-1}\text{)}, \qquad (8)$$

for Brownian motion. This work seeks to utilize Eq (8) for assessing the convergence of $T_n(t)$.

For a function $g(t)$, power spectrum can be formally expressed as

$$S_g(f) = \lim_{P\to\infty}\frac{1}{2P}\left|\int_{-P}^{P} g(t)e^{-i2\pi ft}dt\right|^2, \qquad (9)$$

where i is the imaginary unit ($i^2=-1$). If the observation of $g(t)$, which is denoted as $\hat{g}(t)$, is available only for $0\le t\le 1$, Eq (9) is approximated as

$$S_g(f) \approx \left|\int_0^1 \hat{g}(t)e^{-i2\pi ft}dt\right|^2 \qquad (10)$$

by assuming that $\hat{g}(t)$ on [0,1] is extended periodically to $\mathbb{R}$. As $T_n(t)$ in Eq (4) is obtained for $0\le t\le 1$ in one MC calculation, the power spectrum of $T_n(t)$ is computed using Eq (10) as

$$S_{Tn}(f) = \left|\frac{1}{n}\sum_{m=1}^{n-1} T_n\left(\frac{m}{n}\right)\exp\left(-i\frac{2\pi fm}{n}\right)\right|^2. \qquad (11)$$

Here, the summation over m is 1 through $n-1$ because of $T_n(0)=T_n(1)=0$. The power spectrum of Brownian bridge on [0,1] is also formally expressed as

$$S_{BB}(f) = \left|\int_0^1 B_B(t)e^{-i2\pi ft}dt\right|^2. \qquad (12)$$

For Eqs (11) and (12), the convergence theorem in Eq (4) implies

$$S_{Tn}(f) \to S_{BB}(f)\ \text{ as }\ n\to\infty. \qquad (13)$$

Therefore, it is worthwhile arguing whether or not $S_{BB}(f)= S_{BM}(f)$ since $S_{BM}(f)$ is known as in Eq (8).

On the domain of Brownian bridge [0,1], the difference between Brownian motion and Brownian bridge is $tB_M(1)$. Its Fourier transform is proportional to

$$\int_0^1 te^{-i2\pi ft}dt = \frac{e^{-i2\pi f}}{(-i2\pi f)} - \frac{e^{-i2\pi f}-1}{(-i2\pi f)^2}. \qquad (14)$$

As it is not possible to see low frequency components from the Fourier transform of time domain values on $0\le t\le 1$, one should restrict attention to $f \gg 1$. This restriction leads to

$$\left|\int_0^1 tB_M(1)e^{-2\pi ift}dt\right|^2 \propto \frac{1}{f^2}\ \text{ for }\ f \gg 1. \qquad (15)$$

The above characteristic implies that the presence of $tB_M(1)$ in $B_B(t)$ does not introduce in $S_{BB}(f)$ a frequency component decreasing slower than $1/f^2$. On the other hand, Brownian motion is a stochastic process with stationary increments, zero mean and scale invariant statistical properties.[10] (In probability theory[11], $B_M(ut) =_d u^{1/2}B_M(t)$ for $u>0$ where $=_d$ stands for equality in distribution.) Therefore, Eq (8) leads to

$$\left|\int_0^1 B_M(t)e^{-2\pi ift}dt\right|^2 \propto \frac{1}{f^2}. \qquad (16)$$

These arguments through Eqs (14)-(16) yield

$$S_{BB}(f) \propto \frac{1}{f^2} \quad \text{for} \quad f \gg 1 . \tag{17}$$

Finally, based on Eqs (13) and (17), one can compute $S_{Tn}(f)$ in Eq (11) to see if

$$S_{Tn}(f) \propto \frac{1}{f^2} \quad \text{for} \quad f \gg 1 \text{ as } n \to \infty , \tag{18}$$

in order to make a judgment on the convergence of tallies in terms of CID. In this work, we compute $S_{Tn}(f)$ for $10 \le f \le 1000$ to see if $\log(S_{Tn}(f))$ decreases at the slope of −2 with respect to $\log(f)$. We also utilize the OWSTS estimator in Eq (7) for the standard deviation of the sample mean of tallies because of the direct relevance to CID as implied in Eqs (4), (6) and (7).

III. UO_2-CONCRETE MODEL WITH MATERIAL DISTRIBUTION UNCERTAINTY

In this work, a preliminary model of UO_2-concrete debris[3] is a demonstration problem for the utility of Eq (18). The model geometry is a cube of 140×140×140 cm^3. Inside this cube, a smaller cube of 100×100×100 cm^3 is situated at center with the corresponding faces parallel to each other. The smaller cube is occupied by concrete and UO_2 fuel at the burnup of 12 GWd/t with the average volume ratio of 7:1 in concrete to fuel. The outside of the smaller cube is occupied by concrete only. Table I below shows one energy group cross sections computed by the MVP code.[12]

Table I. One energy group cross sections in cm^{-1}

material	fuel (F)	concrete (C)
total (Σ_t)	0.45324	0.47736
absorption(Σ_a)	0.07038	0.00159
scattering(Σ_s)	0.38286	0.47577
ν-fission($\nu\Sigma_f$)	0.09551	0.0

Inside the smaller cube, the cross section of reaction-type rt is assigned by

$$\Sigma_{rt}(\mathbf{r}) = [\mathrm{v}(1+\Delta\mathrm{v}(\mathbf{r}))]\Sigma_{rt}^{F} + [1-\mathrm{v}(1+\Delta\mathrm{v}(\mathbf{r}))]\Sigma_{rt}^{C}$$
$$\mathbf{r} \in [0,100]\times[0,100]\times[0,100] \tag{19}$$

where $\mathbf{r}$ is the space coordinates inside the smaller cube, the superscripts F and C correspond to fuel and concrete, v=1/8 is the mean volume fraction of fuel, and Δv($\mathbf{r}$) is the space-dependent variation of the volume fraction of fuel satisfying $-1 \le \Delta\mathrm{v}(\mathbf{r}) \le 1$. In this work, Δv($\mathbf{r}$) is assigned the randomized Weierstrass function (RWF)[13] for the reason argued as follows. In general, statistical information for the spatial distribution of material composition will not be available for the medium formed via molten core concrete interaction (MCCI). However, it is certain that the real MCCI compounds are formed under disorder in uncontrollable situations. It was shown in a quite general context that the dynamical system state reached via extreme disorder can be characterized by $1/f^{1+2\alpha}$ $0<\alpha\le 0.5$ in the frequency domain representation[14] under the consistency requirement for intrinsic random fields.[15] Here, it is worthwhile noting that $\alpha\approx 0$ and $\alpha=0.5$ correspond to the 1/f fluctuation and Brownian motion, respectively, and RWF[13] is known to be a stationary approximation to the stochastic process characterized by $1/f^{1+2\alpha}$ in terms of small separation distances. For these reasons, RWF can be a prime approach of choice when no specific statistical information is available. The explicit expression of RWF for Δv in Eq (19) is

$$\Delta\mathrm{v}(\mathbf{r}) = d\sum_{j=1}^{\infty} B_j \lambda^{-\alpha j} \sin(\lambda^j (\mathbf{r}/R)\bullet\mathbf{\Omega}_j + A_j) \tag{20}$$

where d is the parameter determining the level of fluctuation, B_j are the independent Bernoulli random variables taking ±1 equally likely, $\lambda>1$, R is the scaling factor, $\mathbf{\Omega}_j$ are unit vectors chosen uniformly and independently on the unit sphere at the origin, and A_j are independent random variables uniformly distributed on $[0,2\pi)$. As B_j, $\mathbf{\Omega}_j$ and A_j are independent and the expected value of B_j is zero, the expected value of Δv($\mathbf{r}$) is zero. In practice, when the summation in Eq (20) is truncated at $j=M$, d is chosen to be

$$d = \frac{\lambda^{\alpha}-1}{1-\lambda^{-\alpha M}} \tag{21}$$

so that $-1 \le \Delta\mathrm{v}(\mathbf{r}) \le 1$ is satisfied. Note that Δv($\mathbf{r}$) is strictly upper and lower bounded unlike the modeling with normal and log-normal distributions. In other words, it is not necessary to discard non-physical realizations such as negative and larger-than-100% values.

Outside the smaller cube in the cube of 140×140×140 cm^3, the cross section of reaction-type rt is assigned by

$$\Sigma_{rt}(\mathbf{r}) = \Sigma_{rt}^{C} ,\ \mathbf{r} \notin [0,100]\times[0,100]\times[0,100] . \tag{22}$$

so that 100% concrete is represented.

IV. NUMERICAL RESULTS

In this section, numerical results are demonstrated for the UO_2-concrete model in Section III. A single whole set of

MC criticality calculation, which consisted of 4000 generations and 20000 particles per generation with 1000 skip generations, was conducted using the delta tracking[16] for each of 100 realizations of the RWF replicas for Δv(**r**). In Eq (20), the parameters α, λ and *R* were set 0.5, 1.5 and 25 cm, respectively; the summation was truncated at *M*=23 so that $\lambda^{-\alpha M}$=0.009; the parameter *d* was determined by Eq (21); B_j, $\mathbf{\Omega}_j$, A_j were sampled independently over 100 realizations of the RWF replicas. The standard deviation of the sample mean of effective multiplication factor (k_{eff}) tallies is shown in Fig. 1 for each realization of the RWF replicas. It is seen that the standard deviation estimates obtained by OWSTS (the square root of Eq (7)) are on average larger than the estimates without taking into account correlation. However, the OWSTS estimates appear to be fluctuating about 16% (0.000013/0.000079=0.16). It is strongly desired to clarify whether or not this relatively large fluctuation is due to insufficient convergence in terms of CID.

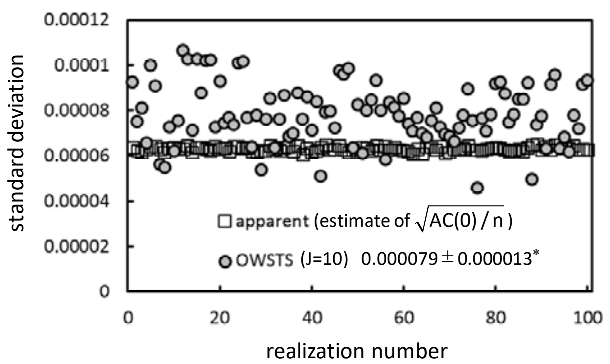

Fig. 1 Standard deviation estimates of effective multiplication factor of UO_2-concrete debris; * for standard deviation of OWSTS estimator for one realization of RWF replica (Δv(**r**)) ; 4000 generations and 20000 particles per generation with 1000 skip generations for one realization

In Fig. 1, the largest estimate of standard deviation is displayed for realization 12. In order to see if the k_{eff} tally in this realization has converged or not in distribution, the power spectrum of ISTS was computed by Eq (11) and is shown in Fig. 2. It is seen that the power spectrum behaves like $1/f^2$ for 10≤f≤1000. Fig. 3 shows the slope of power spectrum for each of 100 realizations of $B_M(t)$ on 0≤*t*≤1. Here, each realization of $B_M(t)$ was computed as follows. First, the covariance matrix of $B_M(t)$, denoted as $\mathbf{C}=(C_{j,k})$, was introduced as[11]

$$C_{j,k} = E[B_M(t_j)B_M(t_k)] = \min(t_j, t_k),$$

$$t_j = \frac{j}{n}, t_k = \frac{k}{n}, \ j,k = 1,\ldots,n. \quad (23)$$

Second, taking into account that covariance matrices are symmetric and non-negative definite, the matrix **C** was factorized into the product of a lower triangular matrix **L** and its transpose $\mathbf{L}^{\mathrm{T}}$ using Cholesky factorization:

$$\mathbf{C} = (C_{i,j}) = \mathbf{L}\mathbf{L}^{\mathrm{T}}. \quad (24)$$

Let $\mathbf{V} \equiv (V_1, V_2, \ldots, V_n)$ be a vector of independent random variables under the standard normal distribution; $E[V_j]$=0, $E[(V_j)^2]$=1 and $E[V_jV_k]$=0 for $j \neq k$ where the subscripts of V_j and V_k corresponds to t_j and t_k. It then follows that the covariance matrix of **LV** becomes equal to $E[\mathbf{L}\mathbf{V}\mathbf{V}^{\mathrm{T}}\mathbf{L}^{\mathrm{T}}] = \mathbf{L}\mathbf{L}^{\mathrm{T}} = \mathbf{C}$. Finally, by sampling $(V_1, V_2, \ldots, V_n)$, $B_M(t)$ on (0,1] was obtained as

$$\left(\hat{B}_M(t_1), \hat{B}_M(t_2), \ldots, \hat{B}_M(t_n)\right) = (\mathbf{LV})^{\mathrm{T}} \quad (25)$$

The number of samples *n* corresponds to the number of generations and was taken to be 5000. Power spectrum was then computed by

$$S_{\hat{B}_M}(f) \approx \left| \frac{1}{n} \sum_{k=1}^{n} \hat{B}_M(t_k) \exp\left(-i2\pi f t_k\right) \right|^2 \quad (26)$$

and its slope was estimated by the least square fitting of $(\log f, \log S_{\hat{B}_M}(f))$ for each of 100 realizations of Eq (25). As displayed in Fig. 3, the slope obtained is −1.99±0.13. This means that the uncertainty of the slope of power spectrum is ±0.13 in one-sigma under CID and thus the result in Fig. 2 indicates CID.

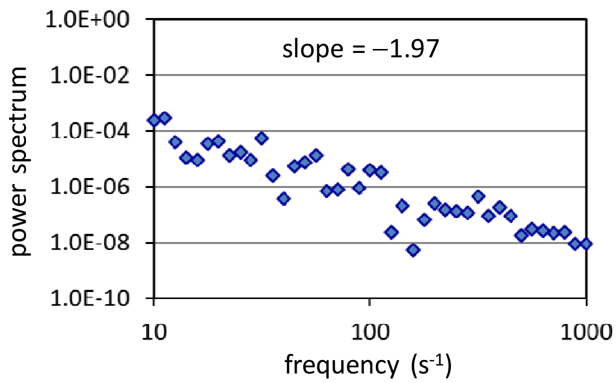

Fig. 2 Largest estimate (replica 12) in Fig. 1 - Power spectrum of interpolated standardized time series of k_{eff} tallies

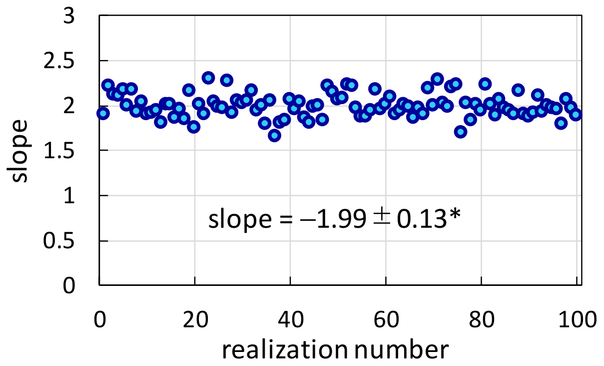

Fig. 3 Slope of power spectrum of Brownian motion on $0 \le t \le 1$; sampling width = 1/5000; * for standard deviation for one realization.

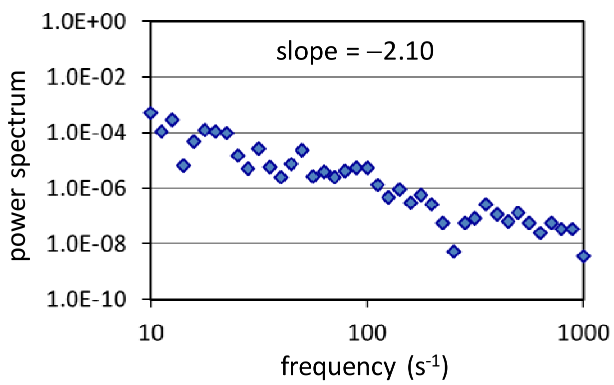

Fig. 4 Almost average estimate (replica 3) in Fig. 1 - Power spectrum of interpolated standardized time series of k_{eff} tallies

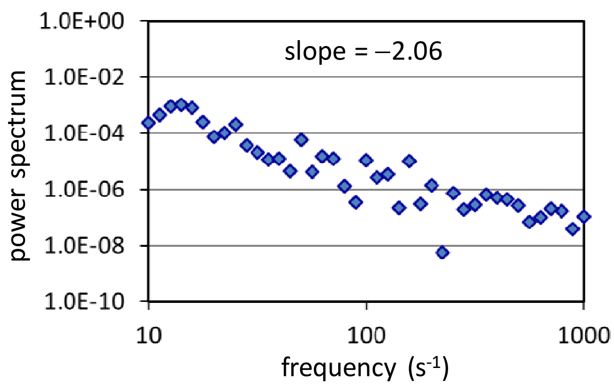

Fig. 5 Smallest estimate (replica 76) in Fig. 1 - Power spectrum of interpolated standardized time series of k_{eff} tallies

Other realizations were also examined and turned out to indicate CID. For example, power spectrum is shown in Figure 4 for realization 3 in Fig. 1 yielding an almost average estimate of standard deviation and the slope obtained is −2.10. Power spectrum is shown in Figure 5 for realization 76 in Fig. 1 yielding the smallest estimate of standard deviation and the slope obtained is −2.06. Both of these slopes agreed with the theoretical value of 2 in one-sigma. Therefore, the fluctuation observed in Fig. 1 can be attributed to the differing characteristics of autocovariances $AC(j)$ over realizations of the RWF replicas.

V. CONCLUSION AND REMARKS

In this work, the review of CLT and OWSTS led to the proposal of the spectral analysis of ISTS for assessing CID. It was demonstrated that via the Fourier transform of ISTS one could compute power spectrum which was to be compared with the inverse-square dependence on frequency as a consequence of the convergence of ISTS toward Brownian bridge. The criterion therein was universal, i.e., problem-independent. This aspect of development is the strength of the proposed methodology.

There are two avenues for future research. First, the reexamination of numerical results in the previous work[4] on a whole PWR core model will be the next step test since the UO_2-concrete model in this work is rather a specialized example problem. Second, technical tools in stochastic differential equations may be pursued in order to transform ISTS to other statistic which will be asymptotically under the law of Brownian motion. Such a pursuit will surely enable one to exploit a range of statistics in Brownian motion. For example, Brownian motion has independent increments, which is amenable to some general and robust estimation and tests.

ACKNOWLEDGEMENTS

Work reported in this article was performed under the auspices of the Nuclear Regulation Authority (NRA) / the Secretariat of NRA of Japan.

REFERENCES

1. P. BILLINGSLEY, "The Lindeberg-Lévy Theorem for Martingales," Proc. Am. Math. Soc., 12, 5, 788-792 (1962).
2. L. SCHRUBEN, "Confidence Interval Estimation Using Standardized Time Series," Operations Research, 31, 6, 1090-1108 (1983).
3. T. UEKI, "Monte Carlo Criticality Analysis under Material Distribution Uncertainty," Journal of Nuclear Science and Technology, 54, 3, 267-279 (2017) http://dx.doi.org/10.1080/00223131.2016.1260066.

4. T. UEKI, "Robust Statistical Error Estimation of Local Power Tallies in Monte Carlo Calculation of Light Water Reactor," Nucl. Sci. Eng., 180, 58–68 (2015).
5. H.J. PARK, H.C. LEE, H.J. SHIM, J.Y. CHO, "Real Variance Analysis of Monte Carlo Eigenvalue Calculation by McCARD for Beavrs Benchmark," Ann. Nucl. Energy, 90, 205-211 (2016).
6. P.D. GRIESHEIMER, B.R. NEASE, "Spectral Analysis of Stochastic Noise in Fission Source Distributions from Monte Carlo Eigenvalue calculations," Prog. Nucl. Sci. Tech., 2, 706-715 (2011).
7. R.D. FOLEY and D. GOLDSMAN, "Confidence Intervals Using Orthonormally Weighted Standardized Time Series," ACM Transactions on Modeling and Computer Simulation," 9, 4, 297-325 (1999).
8. B.B. MANDELBROT and J.W. VAN NESS, "Fractional Brownian Motion, Fractional Noises and Applications," SIAM Review, 10, 4, 422-437 (1968); reprint in B.B. Mandelbrot, Gaussian Self-Affinity and Fractals, Springer-Verlag, New York (2002).
9. I.S. REED, P.C. LEE, T.K. TRUONG, "Spectral Representation of Fractional Brownian Motion in n Dimensions and its Properties," IEEE Trans. Inform. Theory, 41, 5, 1439-1451 (1995).
10. K. FALCONER, Fractal Geometry, 2nd Ed., pp. 267-270, John Wiley & Sons, West Sussex, England (2003).
11. R. Durrett, Probability: Theory and Examples, 2nd Ed., pp. 375-376, WadsWorth Publishing Company, Belmont CA USA (1996).
12. Y. NAGAYA, K. OKUMURA, T. MORI, M. NAKAGAWA, "MVP/GMVP II: General Purpose Monte Carlo Codes for Neutron and Photon Transport Calculations Based on Continuous Energy and Multigroup Methods," JAERI-1348, Japan Atomic Energy Research Institute (2005).
13. T. UEKI, "Fluctuation Modeling of Macroscopic Cross Section with Spatial Correlation," Nucl. Sci. Eng., 178, 16-28 (2014).
14. B.R. FRIEDEN, "Spectral 1/f Noise Derived from Extremized Physical Information," Physical Review E, 49(4), 2644-2649 (1994).
15. V. SOLO, "Intrinsic Random Functions and the Paradox of 1/f Noise," SIAM Journal on Applied Mathematics, 52(1), 270-291 (1992).
16. J. SPANIER, "Two Pairs of Families of Estimators for Transport Problems," SIAM Journal on Applied Mathematics 14(4): 702-713 (1966).